Geochimica et Cosmochimica Acta 393 (2025) 75–85

Contents lists available at ScienceDirect

Geochimica et Cosmochimica Acta

journal homepage: www.elsevier.com/locate/gca

Biomarker ^{14}C evidence for sources and recycling of pre-aged organic carbon in Arctic permafrost regions

Julie Lattaud [a,b,*], Timothy I. Eglinton [a], Negar Haghipour [a,c], Marcus Schiedung [d,e], Lisa Bröder [a]

[a] Biogeoscience Group, Geological Institute, ETH Zurich, Sonneggstrasse 5, 8092, Zurich, Switzerland
[b] Department of Environmental Sciences, University of Basel, Bernoullistrasse 30, 4056 Basel, Switzerland
[c] Laboratory of Ion Beam Physics, ETH Zurich, Otto-Stern-Weg 5, 8093, Zurich, Switzerland
[d] Department of Geography, University of Zurich, Winterthurerstrasse 190, 8057 Zurich, Switzerland
[e] Thünen Institute of Climate Smart Agriculture, Bundesallee 68, 38116 Braunschweig, Germany

ARTICLE INFO

Associate editor: Meixun Zhao

Keywords:
Fatty acids
Permafrost
GDGT
Radiocarbon
Soils
Lake sediments

ABSTRACT

Permafrost thaw has the potential to release ancient particulate and dissolved organic matter that had been stored for thousands of years. Previous studies have shown that dissolved organic matter from permafrost is very labile and can be used by heterotrophic microbes close to the thaw area. However, it is unknown if ancient particulate organic matter can also be utilized. This study aims to investigate whether arctic microbial communities (bacteria and Archaea) incorporate ancient organic matter potentially released from thawing permafrost into their biomass. We compare and contrast the radiocarbon signatures of microbial lipids and higher plant biomarkers (representing terrestrial organic matter) from five soil profiles and seven deltaic lake sediment cores from the Mackenzie River drainage basin, Arctic Canada. In the surface soils, modern to post-modern short-chain fatty acids (SCFA) ages indicate *in situ* microbial production, with differential rates of organic carbon (OC) cycling depending on soil moisture. In contrast, SCFA in deeper soils display millennial ages, which likely represent the microbial necromass preserved through mineral association. In deltaic lakes that are disconnected from the river, generally old SCFA suggests the uptake of pre-aged OC by bacteria. In perennially connected lakes, pre-aged SCFA could originate from *in situ* microbial uptake of old OC or from the Mackenzie River. Higher plant-derived long-chain fatty acids (LCFA) present older radiocarbon ages, reflecting mineral stabilization during either pre-aging in soils (for high closure lakes) or riverine transport (for no and low closure lakes). Archaeal lipids are younger than SCFA and LCFA in high closure lakes, and older in low and no closure lakes, mirroring bulk radiocarbon signatures due to their heterotrophic production. These radiocarbon signatures of bacterial biomarker lipids may therefore reflect microbial incorporation of ancient OC (e.g., derived from permafrost thaw) or exceptional preservation (e.g., through mineral stabilization). Hence, even in relatively high OC environments such as arctic aquatic ecosystems, microbes can rely on ancient OC for their growth.

1. Introduction

Climate warming and related drivers of soil thermal change in the Arctic are expected to alter the distribution and dynamics of organic carbon (OC) contained in perennially frozen grounds – permafrost, by enhancing its thaw (e.g., Schuur et al., 2015). In parallel, changes of the hydrological regime, such as increased snow melt and precipitation, alter the connectivity of permafrost soils with streams, which can further exacerbate the effects of global warming. The reactivity and fate of this newly-thawed organic matter remains poorly understood, yet has important consequences with respect to the direction and strength of climate feedbacks. The potential of thawed organic matter to serve as a substrate for heterotrophic metabolism represents one key factor that is still poorly constrained (e.g., Bardgett et al., 2007; Graham et al., 2012; Miesner et al., 2023; Rieb et al., 2024; Schuur et al., 2023).

Studies from major Arctic rivers show that these large fluvial systems contain predominantly young DOC suggesting either that limited mobilization of thawed permafrost carbon has occurred to date or that it

* Corresponding author.
E-mail address: Julie.lattaud@unibas.ch (J. Lattaud).

https://doi.org/10.1016/j.gca.2025.02.010
Received 9 July 2024; Accepted 6 February 2025
Available online 8 February 2025

has been quickly removed upstream, i.e., close to the place of thaw. Mann et al. (2015) showed that microbes in the Kolyma River Basin (Northeastern Siberia) utilized ancient carbon in permafrost thaw waters and millennial-aged carbon across headwater streams, thereby effectively removing ancient carbon from the DOC pool in the stream waters. In addition, laboratory incubation experiments showed that 20 % to 50 % of permafrost DOC is labile (Drake et al., 2018; Holmes et al., 2008; Liu et al., 2019; Mann et al., 2015, Mann et al., 2012) and as such could be decomposed and released back to the atmosphere as CO_2 or CH_4 from soils, surface waters, or drainages (Cole et al., 2007; Drake et al., 2015; Rieb et al., 2024). In fjord sediments that have low organic carbon content (< 2 %), sedimentary microbial communities have been found to use up to 55 % of petrogenic (radiocarbon-dead) organic matter (Ruben et al., 2023). In black shales, microbial communities assimilate 74 to 94 % of radiocarbon-dead carbon (Petsch et al., 2001), showing that typical knowledge on carbon reactivity versus its age can be challenged in specific environments. Hence, it has been shown that microbial communities can use old carbon for heterotrophic processes. However, it is unknown if such processes are common in environments replete in organic matter, such as in lakes underlain by permafrost.

The radiocarbon (^{14}C) content of OC can provide valuable information about the storage and turnover times of OC in soils, as well as the sources of OC transported and deposited by fluvial systems (e.g., Schuur et al., 2016; Trumbore, 2009; Wild et al., 2019). This can be particularly useful in regions such as the Mackenzie Basin where riverine OC may originate from a mixture of sources that span a large range of OC reservoirs with vastly different turnover times, including radiocarbon-dead OC in sedimentary rocks (petrogenic OC), pre-aged soil and permafrost OC, and modern OC derived from terrestrial and aquatic biological production (e.g.., Goñi et al., 2005; Hilton et al., 2015; Schwab et al., 2020). By studying source-specific biomolecules, i.e., biomarkers, and their specific radiocarbon age it is possible to trace more precisely sources and their specific reservoir times (e.g., Gies et al., 2023). Although biomarker lipids typically comprise less than 1 % of the bulk terrestrial organic carbon pool and thus provide a restricted window into the composition of bulk OC (Jasper and Gagosian, 1993), certain lipid biomarkers have proven valuable tracers of terrestrial OC, i.e., lacustrine and soil-derived OC (e.g., Aichner et al., 2021; Gierga et al., 2016; Uchikawa et al., 2008) and their ^{14}C signatures carry information about terrestrial OC dynamics (e.g., Eglinton et al., 2021; Feng et al., 2015). Long-chain leaf wax fatty acids (LCFA, nC > C_{24}), have been widely used to track higher plant-derived carbon (e.g., Eglinton & Eglinton, 2008). In contrast, their short-chain counterparts (C_{16} to C_{20}) are produced ubiquitously (e.g., Matsumoto et al., 2007; Reiffarth et al., 2016; Sauer et al., 2001). LCFA-^{14}C can thus be used to track an estimate of the combined soil storage and transport time of soil-derived OC (Eglinton et al., 2021) whereas SCFA-^{14}C can show bacterial carbon integration of old OC pools. Isoprenoid glycerol dialkyl glycerol tetraethers (isoGDGTs) are microbial membrane lipids primarily produced in aquatic environments by Archaea (Schouten et al., 2013), which can have heterotrophic or autotrophic metabolism. Their branched counterparts (brGDGTs) can be present in both soils and aquatic settings and are biosynthesized by heterotrophic bacteria (Chen et al., 2022; Halamka et al., 2023).

This study examined the ^{14}C contents (expressed as fraction modern, Fm) of multiple biomolecular tracers (LCFAs; SCFAs; isoGDGT-0 and brGDGTs) of terrestrial and aquatic origin in short (< 2 m) sediment cores from mineral soils and seven lakes from five locations of the Mackenzie Delta region (Northwestern Territories, Canada). These different biomarkers and their corresponding ^{14}C signatures are used to assess the incorporation of different carbon sources into biomass with the overall objective to constrain the sources of carbon accumulating in the delta, and to determine whether microbial communities can metabolize (incorporate) old (potentially permafrost-derived) OC.

2. Material and Methods

2.1. Study area and material

The Mackenzie River Delta region (Fig. 1) is experiencing one of the fastest rates of warming globally, with a temperature increase of approximately 1.5 – 2 °C (particularly during winter and spring) since the mid-20th century (Bonsal and Kochtubajda, 2009; Burn and Kokelj, 2009). One consequence of this warming is the accelerated thaw of the catchment's permafrost which covers 90 % of the Mackenzie River delta region (Gruber, 2012). Permafrost aggradation started in the mid- to late Holocene, between ~ 6 – 1 ka BP (Gorham et al., 2007; Treat and Jones, 2018). Additionally, soil OC accumulation in the Mackenzie River basin has been ongoing since the Late Pleistocene deglaciation (Gorham et al., 2007; Treat and Jones, 2018). Between 1991 and 2016, seasonally thawing surface soil layers (the so-called "active layer") have thickened by 5 – 38 cm near Inuvik, on the eastern flank of the Mackenzie River delta (O'Neill et al., 2019). Already by 2009, the ground in the outer delta was over 2.5 °C warmer than it had been in 1970 (Burn and Kokelj, 2009).

The Mackenzie River Delta is characterized by ~ 49,000 small, shallow lakes (Emmerton et al., 2007). These lakes are connected with the main river channel to different degrees and have been classified into three categories (Lesack & Marsh, 2007): "No closure" lakes are continuously linked to the river, "low closure" lakes have a connection that occurs at least once a year during the freshet, and "high closure lakes", characterized by higher levees, are only connected to the river during strong spring freshets, with recurrence intervals that may be only once per decade. The Mackenzie River carries large amounts of ancient rock-derived or "petrogenic" OC (originating primarily from the Devonian Canol Formation) and pre-aged permafrost OC, varying proportions of which are deposited in lake sediments depending on the degree of lake connectivity (Goñi et al., 2005; Hilton et al., 2015; Kabanov and Gouwy, 2017; Lattaud et al., 2021a; Vonk et al., 2019; Yunker et al., 1993, Yunker et al., 2002). This old OC is transported in the particulate fraction (i.e., as POC), while DOC is usually modern in age (ArcticGro, 2024; Schwab et al., 2020).

Lake sediment cores used for this study were recovered from the Mackenzie River Delta in 2009 as described by Vonk et al. (2015). Seven lakes were selected (Fig. 1, Table 1), based on Lattaud et al. (2021a), who studied a suite of lakes for their sedimentological properties. The latter study found that the degree of lake connectivity has not been stable over time. Specifically, UD-4 was high closure before transitioning to low closure before ca. 1890C.E. (i.e., below 90 cm sediment core depth), while MD-2 was low closure before ca. 1930C.E. (i.e., below 110 cm) and is presently a no closure lake. LD-1 has been extensively studied by Vonk et al. (2016), including ^{14}C measurements on SCFA and LCFA; for this lake, only the glycerol dialkyl glycerol tetraether (GDGT) radiocarbon signatures originate from the present study.

In March 2022, the same lakes were revisited to collect water samples to analyze the ^{14}C content of dissolved inorganic carbon (DIC). Duplicate samples were taken from under ice (surface and bottom waters) and filtered (Sterivex with 0.2 μm pore-size) into pre-poisoned (4 μL Hg_2Cl_2) 12 mL exetainer vials without headspace and stored in the dark.

In addition, five composite surface soils (0 – 15 cm) and two composite deeper soil horizons (45 – 60 cm) near Campbell Hills and the town of Inuvik close to the delta region were analyzed for this study (Fig. 1, Table 1). They were all taken from the seasonally thawed active layer on top of the permafrost, sampled in July/August 2019 and have already been described in the studies of Schiedung et al. (2024, 2022). The sites N1 and N2 are in the lowland of the Great Bear Lake Plain (50 – 70 m a.s.l). The sites N4 and N5 are located at more elevated positions (90 – 105 m a.s.l.). The sites N2 – N4 represent a gradient (580 m length and 40 m elevation difference) along the Campbell Hills facing northwest towards Campbell Lake. All soils are characterized as Cryosols

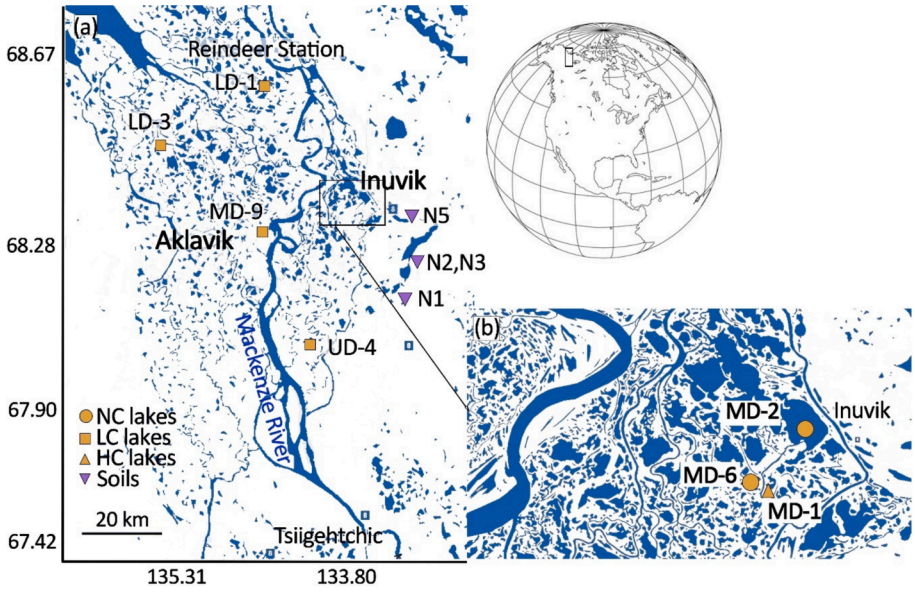

Fig. 1. Location of the studied soils and lakes (a) in the Mackenzie River Delta (*Ehdiitat*) and (b) near Inuvik. NC: no closure, LC: low closure, HC: high closure.

Table 1
Location of the samples.

Name	Latitude (N)	Longitude (W)	Type
MD-1	68.312	133.835	Lake sediment HC
MD-2	68.35843	133.7646	Lake sediment NC
MD-6	68.321	133.861	Lake sediment NC
MD-9	68.26786	134.4795	Lake sediment LC
LD-1	68.67071	134.5658	Lake sediment LC
LD-3	68.481	135.221	Lake sediment LC
UD-4	67.87298	134.1719	Lake sediment LC
N1	68.04222	−113.488	Surface soil
N2	68.16875	−133.434	Surface and deep soil
N3	68.16992	−133.429	Surface soil
N4	68.17236	−133.424	Surface soil
N5	68.31694	−133.533	Surface and deep soil
LD-1 DIC	68.67071	134.56575	Lake water (LC)
MD-1 DIC	68.3119167	133.83535	Lake water (HC)
MD-2 DIC	68.3584333	133.76455	Lake water (NC)
MD-6 DIC	68.3214833	133.8607	Lake water (LC)
MD-9 DIC	68.26786	134.47948	Lake water (LC)
UD-4 DIC	67.87298	134.17191	Lake water (LC)

with turbic (N1 – N3), cambic (N4) and skeletic (N5) properties. Vegetation at moist lowland (mesic to subhygric) sites (N1 and N2) are dominated by black spruce (*Picea mariana*) with a ground cover of dwarf birch (*Betula neoalaskana*). The dryer (subxeric to mesic) sites (N3 – N5) have black spruce and balsam (*Populus balsamifera*) with an undercover of dwarf willow (*Salix herbacea*) (Schiedung et al., 2022). The active layer depth at these sites varied at the time of sampling from 10 to 60 cm. Before analysis, the samples were sieved to < 2 mm, dried at 40 °C and milled for homogenization (Schiedung et al. 2022). For this study, samples from 45 – 60 cm were considered for sites N2 and N5, while 0 – 15 cm was considered for all sites. Composite samples per depth derived from nine individual soil pits (within 30 x 30 m) per site were used for analysis.

2.2. Mineral surface area and bulk radiocarbon measurements

For mineral surface area (MSA), organic matter was removed from a freeze-dried sample aliquot (ca. 1 g) by combustion (12 h, 450 °C, cool-down ramp −40 °C h^{-1}) (Freymond et al., 2018). Before MSA measurement, samples were degassed under vacuum (> 2h, 350 °C) to remove any remaining water and adsorbed gases. MSA was measured with N_2 using the BET method (Brunauer et al., 1938) with a 5-point adsorption isotherm (p/p0 = 0.05–0.3) on a NOVA 4000 surface area analyzer (Keil et al., 1997).

For determination of bulk organic carbon properties, 10 to 15 mg of freeze-dried and homogenized sediment was fumigated with concentrated hydrochloric acid (HCl 37 %) for 72 h at 60 °C to remove inorganic carbon and subsequently neutralized and dried under a basic atmosphere (pH > 7, NaOH) at 60 °C for another 72 h. Radiocarbon isotopic compositions of bulk organic matter were measured with a Mini Carbon Dating System (MICADAS) accelerator mass spectrometer (AMS, Synal et al., 2007), the values are corrected for blank contamination (McIntyre et al., 2016).

Some data were previously published: for LD-1 (all mineral surface area, and bulk Fm) in Vonk et al. (2016, 2019), for some core depths in UD-4, MD-2 and MD-1 (mineral surface area and bulk Fm) in Lattaud et al. (2021a), bulk Fm and LCFA Fm for the soils in Schiedung et al. (2024); the rest originates from this study (see also Tables 1 and 2 for details).

2.3. Lipid extraction and quantification

Freeze-dried sediments from the lakes (5–8 g) and soils (45 g) were extracted with an EDGE system (CEM) as described in Lattaud et al. (2021a). Following extraction, the total lipid extract was saponified with 0.5 M KOH in methanol (MeOH) and the neutral fraction was liquid–liquid extracted three times with hexane. The remaining saponified products were acidified (pH ~1) and fatty acids were liquid–liquid extracted three times with hexane: dichloromethane (DCM) (4: 1, *v/v*). The acid fraction was then methylated overnight 12 h at 70 °C with MeOH: hydrochloric acid (95: 5, *v/v*) of known isotopic composition, and the resulting fatty acid methyl esters (FAMEs) were liquid–liquid extracted four times with hexane. FAME quantification using GC-FID has been described in Lattaud et al. (2021a). To quantify the compounds, a known amount of C_{36} *n*-alkane was run multiple times as external standard during the same sequence. The neutral fraction was separated into three fractions over activated silica oxide column, the most polar fraction eluted with DCM: MeOH (1: 1, *v/v*) containing the GDGTs. The polar fraction was then filtered using a polytetrafluoroethylene 0.45 μm filter prior to analysis.

2.4. Radiocarbon analysis

FAMEs: One to four depths per lake were chosen for radiocarbon analysis depending on FAME concentration. Prior to compound-specific ^{14}C analysis, FAMEs were separated into two "long-chain" fractions (Fraction 1: C_{24-26} and Fraction 2: $C_{28-30-32}$) and a "short-chain" fraction (Fraction 3: C_{16-20}) using a preparative capillary gas chromatography (PCGC) as described in Feng et al. (2015). In brief, the PCGC system consists of a gas chromatograph (GC; Agilent 6890 S) coupled to a Gerstel preparative fraction collector (Gerstel PFC) with a VF-1MS column (30 m × 0.53 mm i.d., film thickness, 0.50 μm). Approximately 10 – 100 μgC of individual target compounds were collected after up to 70 injections on the PCGC (the mass of measured compounds is reported in Supplementary Table 2). A small aliquot of the isolated compounds was used to check purity on a HP 7890A gas chromatograph (GC) equipped with a flame ionization detector (FID), and a VF-1 MS capillary column (30 m × 0.25 mm, 0.25 μm film thickness). The temperature program started with a 1 min hold time at 50 °C, followed by a 10 °C min^{-1} ramp to 320 °C and a 5 min hold time at 320 °C. All fractions were found to yield purities > 99 %, recovery of the PCGC was on average 70 %.

GDGTs: GDGTs were isolated from the polar fraction of the neutral lipids using semi-preparative normal phase high performance liquid chromatography (HPLC) following the method of Gies et al. (2021). Fractions were collected from 16 to 18 min for isoGDGT-0 and 36 to 48 min for the brGDGTs. A small aliquot of the isolated compounds was used to check purity on the same HPLC system and samples with > 95 % purity were subsequently submitted for ^{14}C analysis. The mass of measured compounds is reported in Supplementary Table 2. The soils did not contain sufficient GDGTs for ^{14}C measurement (recommended mass 15 μg, Haghipour et al., 2018).

DIC: An aliquot of 6 mL was subsampled and the headspace was purged with helium for 3 min at 100 mL min^{-1} and acidified with 150 μL of phosphoric acid (85 %) to pH < 2. The ^{14}C composition was measured on a gas-ion source Mini radioCarbon Dating System (MICADAS) accelerator mass spectrometry (AMS) system at the Laboratory for Ion Beam Physics, ETH Zurich (Ruff et al., 2010; Wacker et al., 2010).

Radiocarbon contents of the fatty acids were corrected for derivative carbon (from the methylation step, Fm of the methyl group = 0.004 ± 0.001), and measured $^{14}C/^{12}C$ ratio are reported as fraction modern (Fm, Stuiver and Polach, 1977), and conventional ^{14}C age (Table 1, Supplementary Tables S1, S2). To assess procedural blanks, chemical extraction and PCGC/prep-HPLC isolations were carried out with only solvents and reagents exactly as the samples were run. Radiocarbon-dead (Fm = 0) and modern standards of C_{28} and C_{32} fatty acid for the fatty acids (Fm modern = 1.07) and oxalic acid II (NIST SRM 4990C) and phthalic anhydride (Sigma, PN-320064–500 g, LN-MKBH1376V) for the GDGTs (Fm modern = 1.34) were used to assess carbon contamination. The Fm of the fatty acid solvent blank was 0.89 ± 0.015 (mass = 1.8 ± 0.06 μg). The Fm of the GDGT solvent blanks was 0.52 ± 0.08 (1st sequence) and 0.58 ± 0.01 (2nd sequence) with a mass of 3.10 ± 0.04 μg and 0.88 ± 0.02 μg, respectively, in line with previous contamination assessment (Birkholz et al., 2013; Gies et al., 2021; Shah and Pearson, 2007). All radiocarbon values are corrected for procedural blanks with the errors propagated (Haghipour et al., 2018).

3. Results

3.1. Bulk properties

Bulk lake sediment OC ^{14}C signatures vary between Fm values of 0.20 (LD-1 24–29 cm, data from Vonk et al., 2016; no uncertainties were reported) and 0.83 (MD-1 35–37 cm, data from Lattaud et al., 2021a, Table 2). On average, bulk OC in no closure lake sediments exhibits lower Fm (ave. 0.20 ± 0.04, n = 5) than in high closure lakes (ave. Fm 0.73 ± 0.03, n = 4), while low closure lakes show intermediate values with an average Fm value of 0.41 ± 0.16 (n = 9) (Fig. 2A). Mineral surface area varies from 15.0 ± 0.7 to 25.9 ± 0.3 m^2 g^{-1} (Fig. 3A). The highest MSA values are found in no closure lakes, on average 23.4 ± 1.7

Table 2
Fraction modern (Fm) values and associated measurement error for the bulk sediment and compounds extracted from the lakes and soils (N2 and N5 deep are the 40 – 65 cm deep soil layers). (1) refers to Vonk et al. (2019) and (2) refers to Schiedung et al. (2024).

		Fm						Error Fm					
Name	Depth (cm)	Bulk	FA C_{16-20}	FA C_{24-26}	FA C_{28-30}	GDGT- 0	BrGDGT	Bulk	FA C_{16-20}	FA C_{24-26}	FA C_{28-30}	GDGT- 0	BrGDGT
MD-1	4–7	0.78	0.74	0.80	0.71			0.006	0.007	0.007	0.008		
MD-1	8–10					0.85	0.90					0.023	0.007
MD-1	10–11	0.77	0.82	0.81	0.71		0.79	0.006	0.009	0.008	0.008		0.010
MD-1	24–26	0.75	0.78	0.88	0.80		0.49	0.006	0.000	0.000	0.000		0.074
MD-1	27–29			0.86	0.79					0.007	0.008		
MD-1	30–32	0.82	0.70	0.78	0.66	0.81	0.84	0.007	0.007	0.007	0.007	0.031	0.008
MD-1	35–37	0.83	0.84	0.85	0.82			0.007	0.019	0.008	0.010		
MD-2	27–33	0.27	0.76	0.59				0.003	0.052	0.021			
MD-2	50–59	0.34	0.62	0.58	0.37			0.004	0.025	0.012	0.012		
MD-2	78–97	0.27		0.50	0.29			0.004		0.000	0.000		
MD-6	2–6	0.38	0.66	0.57	0.64	0.34	0.46	0.004	0.007	0.006		0.015	0.006
MD-6	14–19	0.33	0.62	0.54	0.43	0.49	0.40	0.004	0.007	0.006	0.005	0.073	0.005
MD-9	2–6	0.68	0.88	0.51	0.88			0.006	0.008	0.005	0.008		
MD-9	14–19	0.40	0.57	0.67	0.63		0.46	0.004	0.006	0.008	0.008		0.007
LD-1	14–19	0.20(1)			0.51(1)	0.25	0.32					0.006	0.006
LD-1	24–29	0.20(1)			0.53(1)	0.24	0.31					0.007	0.004
LD-3	1–6	0.53	0.76	0.72	0.32	0.53	0.67	0.005	0.007	0.007	0.004	0.009	0.008
LD-3	14–19	0.37	0.48	0.61	0.31			0.004	0.006	0.006	0.004		
UD-4	0–4	0.54	0.78	0.76	0.63			0.007	0.009	0.007	0.008		
UD-4	10–19	0.33	0.80		0.40			0.004	0.008		0.006		
UD-4	20–29	0.51	0.89	0.75	0.68	0.46	0.54	0.006	0.013	0.010	0.011	0.095	0.075
UD-4	86–98	0.76	0.80	0.64	0.45			0.007	0.008	0.007	0.007		
N1	0–15	0.78(2)	0.85	0.86	0.84(2)			0.01(2)	0.010	0.013	0.004		
N2	0–15	0.78(2)	0.89	0.89	0.88(2)			0.01(2)	0.007	0.007	0.002		
N3	0–15	0.85(2)	0.90	0.89	0.80(2)			0.01(2)	0.007	0.007	0.001		
N4	0–15	0.88(2)	0.98	0.97	0.91(2)			0.01(2)	0.007	0.007	0.002		
N5	0–15	0.90(2)	1.06	0.98	1.00(2)			0.01(2)	0.008	0.007	0.002		
N2 deep	45–60	0.56(2)	0.76	0.72	0.73(2)			0.00(2)	0.008	0.007	0.002		
N5 deep	45–60	0.39(2)	0.82	0.74	0.70(2)			0.00(2)	0.029	0.015	0.009		

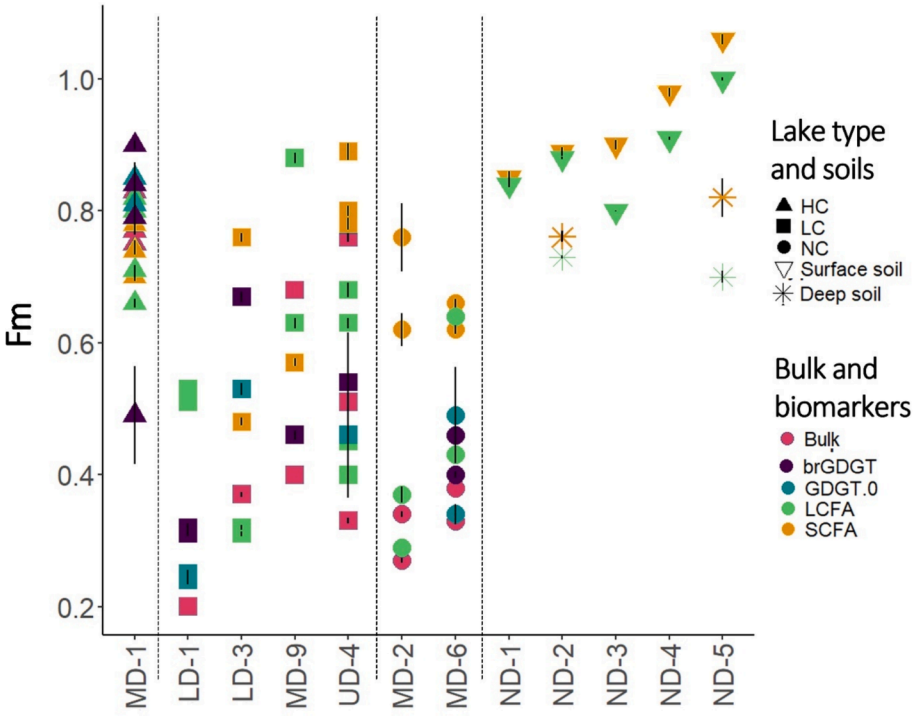

Fig. 2. Fraction modern (Fm) of specific biomarkers and bulk organic carbon, organized by lake types. All depth within the sediment cores or soil profiles are plotted together. LCFA. LCFA ages in the soils are from Schiedung et al. (2024). Error bars indicate measurement uncertainties and blank correction.

$m^2\ g^{-1}$ (n = 5, 2 lakes), which also have more clay content (Fig. 3C, Lattaud et al., 2021a) than high closure lakes (ave. 17.4 ± 1.4 $m^2\ g^{-1}$, n = 6, 1 lake) and low closure lakes (ave. 18.4 ± 2.4 $m^2\ g^{-1}$, n = 9, 4 lakes). These findings are in agreement with previous results of Lattaud et al. (2021a). The intra-lake MSA variability is up to 4 $m^2\ g^{-1}$.

Fm values of DIC in the lake waters (in 2022) varies from 0.83 in the bottom of LD-1 to 0.99 at the bottom of MD-2 and surface of MD-9 (Fig. 3D, Supplementary Table 3) with an average Fm value of bottom and surface DIC of 0.91 ± 0.06 (n = 11). In comparison, in the Mackenzie River, DIC Fm values vary from 0.83 to 0.88 (ave. 0.85 ± 0.02, n = 5) (Fig. 3D, Dasari et al., 2024).

3.2. Sediments and soils concentrations and radiocarbon values of FA

SCFA concentrations in the soils vary from 0.01 to 0.03 ug g_{sed}^{-1} for the surface soils, up to 0.03 μ g g_{sed}^{-1} in the N2 deep layer. LCFA concentrations range between 0.001 and 0.020 μ g g_{sed}^{-1}. In the lakes, SCFA concentrations are highest in MD-1 (32 to 90 μ g g_{sed}^{-1}) and lowest in LD-1 and MD-6 (0.8 μ g g_{sed}^{-1} and ave. 0.87 ± 0.19 μ g g_{sed}^{-1}, respectively). LCFA are also highest in MD-1 (30 to 101 μ g g_{sed}^{-1}).

Radiocarbon signatures of LCFA ($C_{24\text{-}26\text{-}28\text{-}30}$) from lake LD-1 have been described in Vonk et al. (2019). Here, we summarize results for the other lakes (see also Table 2):

MD-1 (High closure): Fm values of FA vary from 0.66 for the $C_{28\text{-}32}$ at 30–32 cm to 0.88 ($C_{24\text{-}26}$ at 23–24 cm) (Fig. 4). The average Fm values of the SCFA ($C_{16\text{-}20}$), and LCFA ($C_{28\text{-}30\text{-}32}$), respectively, are 0.78 ± 0.05 (n = 4), and 0.75 ± 0.06 (n = 4) (Fig. 2). Fm of the LCFA lower than the shorter chain counterparts (< C_{26}), while Fm of the $C_{24\text{-}26}$ FA are systematically higher (although equivalent to $C_{16\text{-}20}$ FA for the 10 –11 cm depth interval). The depth interval 35 – 37 cm yielded the higher Fm of all FA.

LD-3 (Low closure): Fm of FA varies from 0.31 ($C_{28\text{-}30}$ at 14 – 19 cm) to 0.76 ($C_{16\text{-}20}$ at 1 – 6 cm) (Fig. 2). On average, $C_{16\text{-}20}$ Fm values are 0.62 ± 0.14 (n = 2), $C_{24\text{-}26}$ Fm values are 0.66 ± 0.06 (n = 2), $C_{28\text{-}30}$ Fm values are 0.31 ± 0 (n = 2) (Fig. 2).

MD-9 (Low closure): Fm of FA varies from 0.514 ($C_{24\text{-}26}$ at 2 – 6 cm) to 0.881 ($C_{16\text{-}20}$ at 2 – 6 cm) (Fig. 2). On average, $C_{16\text{-}20}$ Fm values are 0.73 ± 0.15 (n = 2), $C_{24\text{-}26}$ Fm values are 0.59 ± 0.08 (n = 2), and $C_{28\text{-}30}$ Fm values are 0.75 ± 0.13 (n = 2) (Fig. 2). Fm gets lower with depth for SCFA and LCFA.

UD-4 (Low closure): Fm of FA varies from 0.40 ($C_{28\text{-}30}$ at 10–19 cm) to 0.89 ($C_{16\text{-}20}$ at 22–23 cm) (Fig. 2). Fm values are on average 0.82 ± 0.04 ($C_{16\text{-}20}$, n = 4), 0.72 ± 0.05 ($C_{24\text{-}26}$, n = 3) to 0.54 ± 0.1 ($C_{28\text{-}30\text{-}32}$, n = 4) for SC, MC and LC FA, respectively (Fig. 2). Fm of the SCFA are systematically higher than $C_{24\text{-}26}$, which are in turn higher than the LCFA. There is no trend with depth, except for the Fm of the $C_{24\text{-}26}$ that increase with depth.

MD-2 (No closure): Fm of FA varies from 0.29 ($C_{28\text{-}32}$ at 78–97 cm) to 0.76 ($C_{16\text{-}20}$ at 27 – 33 cm) (Figs. 2, 4). Fm values generally decrease with increasing FA chain length, averaging 0.69 ± 0.07 ($C_{16\text{-}20}$, n = 3) and 0.33 ± 0.04 ($C_{28\text{-}30\text{-}32}$, n = 2) for short and long FA, respectively (Fig. 2). The SCFA (< C_{20}) have a systematically higher Fm than the longer chain homologues and all Fm of the FA become lower with increasing depth.

MD-6 (No closure): Fm of FA varies from 0.54 ($C_{24\text{-}26}$ at 14 – 19 cm) to 0.92 ($C_{16\text{-}20}$ and $C_{28\text{-}32}$ at 14 – 19 cm) (Fig. 2). In average, $C_{16\text{-}20}$ Fm values are 0.64 ± 0.02 (n = 2), $C_{24\text{-}26}$ Fm values are 0.56 ± 0.02 (n = 2), $C_{28\text{-}30}$ Fm values are 0.53 ± 0.10 (n = 2) (Fig. 2).

Soils: Fm values of the LCFA ($C_{28\text{-}30}$) have been reported in Schiedung et al (2024) and vary between 0.84 ± 0.01 in the surface soils of N1 and 1.00 ± 0.01 in the surface soils of N5 (Fig. 2). Fm of the SCFA ($C_{16\text{-}20}$, this study) are systematically higher than the longer chain counterparts (the offset translates in ^{14}C ages between 1000 and 100 years) and vary between 0.85 ± 0.01 and 1.06 ± 0.01 (bomb-spike influenced, post-modern) (Fig. 2). The Fm of the $C_{24\text{-}26}$ FA (this study) are similar to those of the SCFA. In the deeper layers, the SCFA are about 1300 – 2000 years older than in their respective values for the surface soil.

3.3. Concentrations and radiocarbon values of GDGTs

The radiocarbon content of isoGDGT-0 was measured in 8 sediment samples (five different lakes) and branched-GDGTs (brGDGTs) in 11

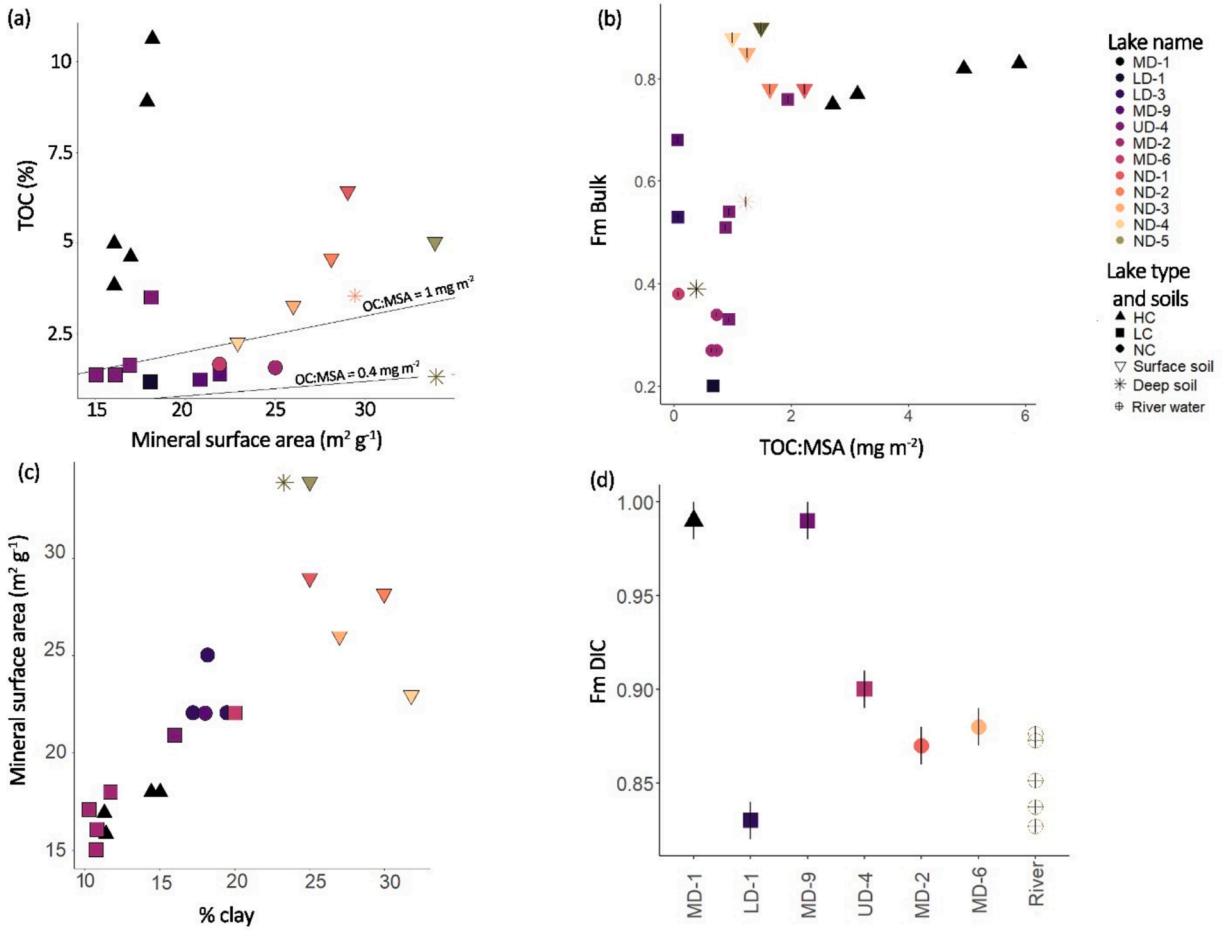

Fig. 3. Lake and soil bulk properties (a) mineral surface area (MSA) and total organic carbon (TOC) and (b) the ratio of TOC against MSA and Fm of bulk OC, (c) mineral surface area and percentage of clay (data from Schiedung et al., 2022; Lattaud et al., 2021a), and (d) Fm of DIC of surface lake water, and Mackenzie River water (n = 6, from 2013 and 2017) from Dasari et al. (2024). Error bars indicate measurement uncertainties and blank correction.

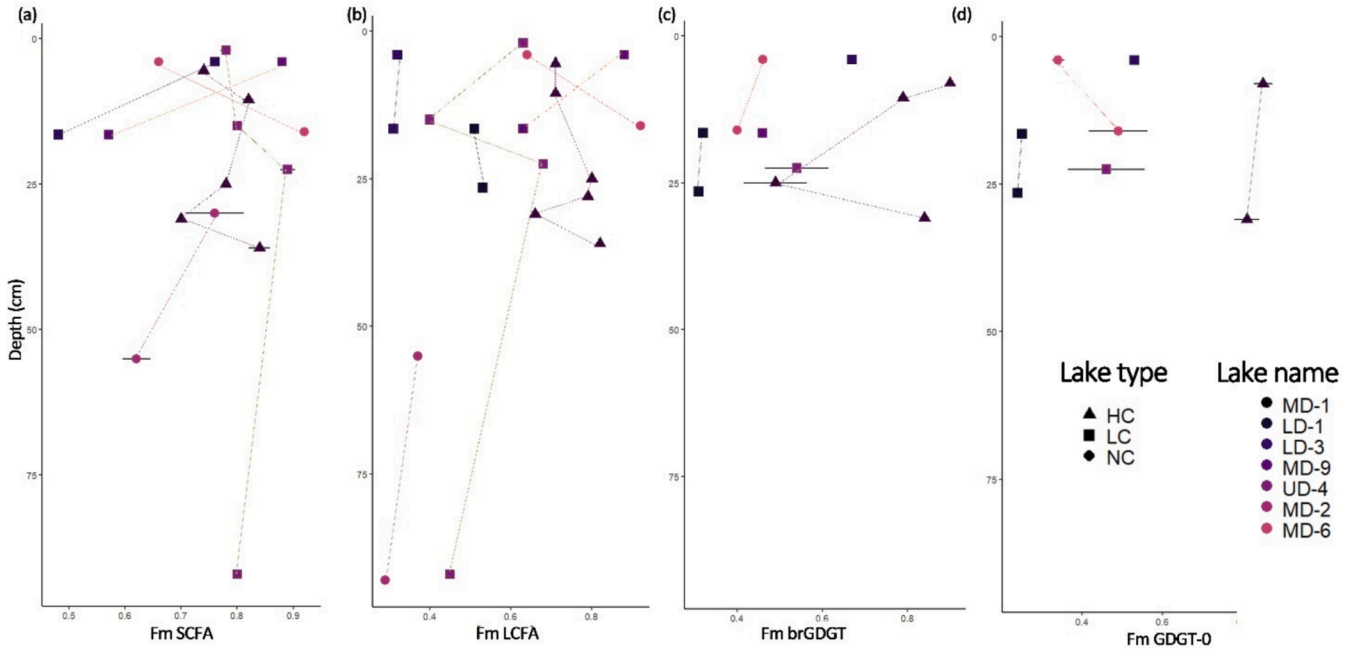

Fig. 4. Downcore biomarker fraction modern, Fm, (a) short-chain fatty acids, SCFA, (b) long-chain fatty acids, LCFA, (c) branched glycerol dialkyl glycerol tetraether, brGDGT and (d) isoprenoid glycerol dialkyl glycerol tetraether 0, isoGDGT-0. Error bars indicate measurement uncertainties and blank correction.

samples (six different lakes). The limited number of measurements is due primarily to analytical requirements (>10 μg C is needed for robust ^{14}C measurements, Gies et al., 2021), and low GDGT abundances, especially in soils (2 – 14 ng g^{-1}) that precluded radiocarbon analysis.

Fm values of brGDGTs vary from 0.31 (LD-1 at 24 – 29 cm) to 0.90 (MD-1 at 7 – 10 cm) (Figs. 2, 4). For the lakes with ^{14}C data from more than one sediment depth (three different lakes), for two out of three measurements, the upper depth interval yields a higher Fm value (younger brGDGT ^{14}C age, Fig. S1) than the lower interval (e.g., MD-6 at 2 – 6 cm whereas at 14 – 19 cm). For MD-1, Fm of the deeper layer at 30 – 32 cm is higher than the above-sampled layer (Fig. 4). This lower layer developed prior to the shift in sediment properties that was linked to a change in lake connectivity to the river and likely was a peat deposit at that time (Lattaud et al., 2021a). GDGT-0 Fm varies from 0.24 (LD-1, 24 – 29 cm) up to 0.85 (LD-3, 1 – 6 cm) (Figs. 2, 4).

4. Discussion

In all but the high closure lakes, OC loadings are between the 0.4 – 1 mg C m^{-2} indicating classic river-suspended material (Fig. 3A, Blair and Aller, 2012). In the high closure lake and most soils, these loadings are above 1 mg C m^{-2} (Fig. 3A), indicating higher OC production and/or more efficient preservation. Younger bulk ^{14}C OC in the high closure lake and soils (0.78 < Fm < 0.90, Fig. 2) confirm the greater production/preservation of more modern OC, whereas low and no closure lakes have a much older bulk ^{14}C OC (Fm < 0.76), indicating input of petrogenic or extensively pre-aged carbon (Drenzek et al., 2007). Given the potential influence of petrogenic carbon on bulk carbon signatures, ^{14}C measurements on more source-specific components, i.e., biomarkers, are needed to better understand different source contributions and their respective dynamics and turnover times.

4.1. Origin of aged short-chain fatty acids in soils

SCFA are labile and ubiquitous compounds (e.g., Matsumoto et al., 2007; Reiffarth et al., 2016; Sauer et al., 2001), and they are thought to degrade relatively quickly in comparison to their long-chain counterparts (e.g., Eglinton et al., 2021; Kusch et al., 2021; Parker et al., 2023; Vonk et al., 2019). Hence, their presence in soils and sediments likely predominantly reflects *in situ* production of a fast cycling pool of OC (Van Der Voort et al., 2017). In the surface soils of the Mackenzie Delta, SCFA likely stem from a mixture of inputs, including bacterial production, root organic matter and stabilized plant organic matter (Gies et al., 2021; Reiffarth et al., 2016; Simoneit, 2005; Van Der Voort et al., 2017; Wiesenberg et al., 2010). Post-modern SCFA are found in the elevated and dry soils (Fm = 1.06 and 0.98; post-modern age, N5 and N4), implying the predominance of young (decadal) OC. The oldest SCFA in soils (Fm = 0.85, 1320 ± 80 ^{14}C-yr, Fig. 2) are found in the soils of lowland regions of the Great Bear Lake Plain (N1 and N2; Fig. 1). N1 and N2 are characterized by outwash deposits of Cretaceous shale and Devonian limestone, as well as relicts of Yedoma formations. However, it is unlikely that SCFA originate from these old deposits due to the low amount of SCFA in sedimentary rocks (Drenzek et al., 2009). Similarly, due to the age of the SCFA (> 100 yr in all soils but N5) that outlast usual plant life (Wiesenberg et al., 2010), it is unlikely that they originate from root-OM. It is possible that some heterotrophic microbes take up petrogenic or old pyrogenic OC, which is expected to be present in these soils (Schiedung et al., 2024). However, these OC pools are generally thought to be relatively recalcitrant, thus withstanding microbial degradation (Bird et al., 2015; Blair et al., 2003). Uptake of old OC has so far only been demonstrated in areas lacking fresh OC (e.g., Drenzek et al., 2009; Horan et al., 2019; Petsch et al., 2001; Ruben et al., 2023), which is unlikely in the soils here as they contain 2.0 – 6.4 % OC (Schiedung et al., 2022). Hence, in all soils but N5, SCFA radiocarbon signatures likely reflect preservation processes, i.e., stabilization through OC-mineral interactions in the soil (c.f., Van Der Voort et al. (2017) or due to environmental conditions favourable for OC preservation (such as low ambient temperatures, anoxia, higher pH, moisture content). The mineral surface area is slightly lower in the moist lowland sites (28 – 29 m^2 g^{-1}), mean grain size is slightly higher (17 – 14 % sand, 50 – 52 % silt), and SCFA concentration are higher (34 ng $gsed^{-1}$) compared with the dry elevated sites (34 – 23 m^2 g^{-1}, 15–12 % sand and 58 – 55 % silt and 35 ng $gsed^{-1}$), suggesting higher preservation potential (through association with mineral surfaces) for the dryer elevated sites. However, the fraction of total soil OC found to be mineral associated OC in the lowland and elevated sites are similar (41 – 88 % and 42 – 54 % respectively; Schiedung et al., 2023). This gradient in SCFA radiocarbon content (Fm) from elevated sites to lowlands, which is also reflected in the bulk OC ^{14}C (Schiedung et al., 2024), may instead be due to the difference in soil moisture content at the sites, which has been shown to exert primary control on OC cycling in mineral soils underlain by permafrost (Schiedung et al., 2022). Specifically, OC appears to be better preserved at the dryer elevated sites where microbial decomposition is inhibited, whereas increased accumulation of aged and residual OC occurs at moist lowland sites due to the faster recycling of freshly produced organic matter (Schiedung et al., 2022, 2024). The latter process would prevent the preservation of fresh modern SCFA and could explain our observations of older SCFA for site N1. The SCFA present in the deeper soils are significantly older than in the surface soils of the respective sites (> 45 cm depth, at N2 Fm = 0.76 ± 0.01, and at N5 Fm = 0.82 ± 0.03, Fig. 2), suggesting that at greater soil depth there is less input of modern OC and that only the millennial-pool of stabilized SCFA persists (Van Der Voort et al., 2017). In comparison, LCFA are systematically older than the SCFA by ~ 400 yr for all sites and depths (Fig. 2) and therefore could represent a slower cycling pool (e.g., Van der Voort et al., 2017). LCFA are thought to be more recalcitrant than SCFA and readily interact with mineral surfaces, thereby limiting their degradation by microbial communities (Hemingway et al., 2019; Keil et al., 1994; Van Der Voort et al., 2017).

4.2. Source(s) of pre-aged short-chain fatty acids in deltaic lake sediments

The Mackenzie Delta lakes are characterized by strong macrophyte and bacterial production in summer (Squires and Lesack, 2002). Algal blooms are infrequent, restricted by either very high turbidity from Mackenzie River waters to no and low closure lakes, or the high accumulation of macrophytes at the surface of high closure lakes (Tranvik et al., 2009). In the high closure lake MD-1, SCFA in the (sub)surface sedimentary layer (4 – 7 cm) are about 400 years older than the surface sedimentary bulk OC and about 2400 years older than the SCFA in surface soil horizons, yet similar to those of deeper soil horizons in the surrounding catchment area (Fig. 2, Table 2). It should be noted, however, that these soils are distal from the lake (Fig. 1). Over the length of the core (38 cm), covering the period from 1813 to 2003 (with an average sedimentation rates of 0.2 cm yr^{-1}, Lattaud et al., 2021a), there is no clear age-depth increase of the SCFA ages (Fig. 4A). Sediment bioturbation can be ruled out as a potential cause as the ^{137}Cs peak is present in the core (Ferguson, 1990; Lattaud et al., 2021a). Similarly, hardwater effects that might contribute to ^{14}C-depleted signatures from aquatic biomass (e.g., macrophytes) can be excluded because present-day DIC ^{14}C-ages in this lake are relatively modern (80 to 205 ^{14}C-yrs, surface and bottom water in winter 2022, Fig. 3D). Instead, the persistently old SCFA throughout the core could stem from input of pre-aged, allochthonous SCFA. Potential sources of millennial-age SCFA are erosion of the deeper soil layers, thawed permafrost-derived SCFA, and heterotrophic microbial consumption of old OC (from permafrost or shales, Petsch et al., 2001; Ruben et al., 2023). Permafrost in the Mackenzie region formed prior to 12 kyr BP (Gruber, 2012). Assuming a simple mixing of two endmembers (Table S3), either 1) modern macrophyte SCFA (the main modern carbon source in the lakes, Fm = 1) and an older carbon source for bacterial communities originating from

2a) 12 kyr-old permafrost OC (Fm = 0.225) or 2b) petrogenic OC (Fm = 0), would yield a contribution of 21 to 38 % of permafrost-thawed OC or 16 to 29 % petrogenic OC into the SCFA pool. These values based on SCFA imply significant bacterial uptake of old OC accumulating in deltaic lake sediments. DOC from thawed permafrost, which could also serve as a source of pre-aged OC to heterotrophic bacteria, is respired close to the permafrost thaw zone while permafrost POC remains within aquatic networks (Bröder et al., 2021; Drake et al., 2018; Keskitalo et al., 2021; Mann et al., 2015).

SCFA in no– and low-closure lakes are similar or older than those in the high-closure lake, and are much older than those in both surface and deep soils (Fig. 2, Table 2). SCFA ages in the Mackenzie River particulate organic carbon pool have been reported to be modern (Feng et al., 2015) and are thus an unlikely source of aged SCFA to the lakes. However, as that study analysed a sample from one time-point only, it does not capture seasonal variability in the material carried by the Mackenzie system. It remains possible, therefore, that older SCFA could be mobilized from deeper soil layers during the spring flood, as also inferred based on SCFA ^{14}C ages of ~ 11 000 yr for the Colville River (Feng et al., 2015). It is not possible to discern clear depth trends in the cores due to the low number of samples per core (n = 2 for all but UD-4 and MD-1). In the core profile from a low closure lake (UD-4), SCFA seem to be uniformly pre-aged (ave. Fm 0.82 ± 0.04, n = 4), very similar to the SCFA ^{14}C content of the high closure lake. This implies that, depending on degree of lake connectivity, old SCFA in the Mackenzie Delta lakes may originate from bacterial heterotrophic biomass that utilize pre-aged OC as a carbon source, and/or seasonal fluvial supply (freshet) of pre-aged SCFA.

4.3. Microbial utilisation of pre-aged carbon in deltaic lakes?

To further constrain the carbon sources of lacustrine heterotrophic and autotrophic microbial communities, the radiocarbon signature of GDGTs originating from bacteria (brGDGTs) and Archaea (isoGDGT-0) were determined. Lake sediment brGDGT ^{14}C-ages are younger than corresponding bulk OC (except in one sample in MD-1 where brGDGTs are 3500 yrs older than the bulk ^{14}C age), generally older than LCFA, and uniformly older than SCFA (Fig. 2). The ^{14}C relationship with bulk OC is similar to that observed for Arctic Red River suspended particulate organic carbon (a tributary of the Mackenzie River, Gies et al., 2023), but contrary to previous work in soils (Gies et al., 2021), and marine and lake sediments (Birkholz et al., 2013; Smittenberg et al., 2005). BrGDGTs can be biosynthesized by heterotrophic bacteria either in soils or lake waters (Chen et al., 2022; Halamka et al., 2023; Weijers et al., 2010), and these organisms have been inferred as a source of brGDGTs in the lakes of the Mackenzie Delta (Lattaud et al., 2021b). In high closure lakes, the brGDGT distribution indicates that they predominantly derive from aquatic production (Lattaud et al., 2021b), which is supported by the high Fm values of > 0.80 in three sediment layers of MD-1, while one layer with lower Fm (0.49) points to mixed sources (lake *in situ* production plus either soil or Mackenzie River inputs). In the soil samples, brGDGTs are in low abundance, maybe due to slow OC turnover, not favouring the growth of brGDGT producers (Supplementary Table 3). In the Arctic Red River, one tributary of the Mackenzie River, brGDGTs have been found to have an approximate age of 8000 ^{14}C-yr (Fm = 0.37) during one time-point (Gies et al., 2023), which is older than the lacustrine brGDGTs from this study (except for the low closure lake LD-1). Although, this only represents one time-point (from the spring flood), it provides evidence supporting a mixed origin, i.e. river input and *in situ* production, for brGDGTs.

For the Mackenzie River, dissolved organic carbon (DOC) is generally modern in age, 0.99 ± 0.05 (2009 – 2010) (ArcticGro, 2024) with occasionally older DOC (Fm down to 0.85, Schwab et al., 2020). No DOC radiocarbon signatures are available from the lakes themselves, although in the no and low closure lakes, values are expected to be similar to those of the river (i.e., modern). In the thermokarst high closure lakes such as MD-1, DOC could originate from thermokarst processes and therefore be partly old (Tank et al., 2011). Thus, brGDGT producers might be using old DOC or POC as a carbon source (e.g., Hilton et al., 2015; Vonk et al., 2016). Although POC is less easily accessible by the bacterial pool than DOC, it could originate from permafrost thaw of intrinsically labile organic matter, pyrogenic OC (Schiedung et al., 2024) or petrogenic carbon (Goñi et al., 2005). In addition, mineral stabilisation (Gies et al., 2023) and enhanced preservation in the sediment might also explain the old age of brGDGTs in the no and low closure lakes. LCFA, also considered to be stabilized via mineral association (Van der Voort et al., 2017) are generally younger than brGDGTs in this system, indicating that mineral stabilisation cannot be the only mechanism explaining the relatively old brGDGTs. The alternative explanation remains that aquatic heterotrophic GDGT-producing bacteria in the Mackenzie River and lakes are using old OC sourced from either DOC or POC.

The isoprenoid GDGT, isoGDGT-0, is biosynthesized by diverse Archaea (Schouten et al., 2013). In Mackenzie Delta lakes, Lattaud et al. (2021b) found that this compound is produced by acetoclastic methanogenic or heterotrophic Archaea that utilize acetate or other OC as a carbon substrate. The radiocarbon signatures of this biomarker differ as a function of lake connectivity, with a younger age than SCFA for the high closure lake (MD-1) but older ages relative to these compounds in no and low closure lakes. The ages of isoGDGT-0 in the high closure lake are also similar to bulk OC ages. Although only two samples could be measured for both bulk and compound-specific ^{14}C, the similarities in stable carbon isotopic signals in MD-1 and low closure UD-4 ($\delta^{13}C_{isoGDGT\text{-}0}$ = –22.5 ‰, –26.6 ‰, $\delta^{13}C_{bulk}$ = -24.4 ‰, –25.9 ‰, respectively, Lattaud et al., 2021b) might indicate a heterotrophic *in situ* source rather than methanogenic source for isoGDGT-0. In the high closure lake MD-1, isoGDGT-0 is markedly younger than in the river (isoGDGT-0 in the river has a Fm = 0.27, 10 500 ^{14}C-yr, Gies et al., 2023). An origin from *in situ* aquatic production therefore seems most likely, supported by the sedimentary autochthonous regime of the lake (Lattaud et al., 2021a). The typical Fm values of 0.82 for isoGDGT-0 could either be explained by the metabolism of the heterotrophic archaeal producers that assimilate non-modern bulk OC or by the same community utilizing modern OC (e.g., DOC) with a minor, episodic external (fluvial) supply of more extensively aged isoGDGT-0. In no and low closure lakes, isoGDGT-0 the significantly older radiocarbon ages (by at least 3500 yr) than in the high closure lake likely result from a mixture of contributions from *in situ* production and riverine supply. Assuming a simple two end-member mixing (Table S3) with Fm values for *in situ* production of 0.82 (from the high closure lake) and 0.27 from fluvial supply (Gies et al., 2023), riverine contributions of isoGDGT-0 vary from 28 % (for low closure lake LD-3) to 92 % (for low closure lake LD-1). Overall, the ^{14}C data suggest that a significant fraction of isoGDGT-0 found within deltaic lake sediments reflects the incorporation of aged OC by archaeal producers (either in the river or in the lakes).

4.4. Implications for carbon cycling in Arctic environments

The climatic response to the remobilization of ancient carbon hinges upon the proportion that is respired versus sequestered in sedimentary sinks (e.g., lake or marine sediments). Ancient OC is typically assumed to be refractory since it has already escaped degradation for an extended period of time. However, for permafrost OC this protection is thought to be due to its frozen storage, implying that it may become labile as environmental conditions change (Guillemette et al., 2017). Permafrost thaw thus liberates potentially labile ancient carbon, possibly rendering it available to modern microbial communities, although the extent to which respiration occurs remains unclear. Marine aquatic microbial communities have been shown to dynamically respond to the availability of permafrost carbon (Ruben et al., 2024). Microbial utilization of ancient carbon has also been observed in thaw waters and headwater

streams of the Kolyma River basin in Siberia (Mann et al., 2015). Other studies have shown that only a small proportion of permafrost OC reaches the marine realm (Chen et al., 2016; Elberling et al., 2013; Schädel et al., 2014), indicating that deposition and/or respiration occurs along the land-to-sea aquatic continuum. In the Mackenzie Delta lakes, our results suggest that bacterial communities can use 21 to 38 % of ancient carbon in lipid biosynthesis, suggesting that ancient carbon incorporation into the food web may become prevalent across the Arctic domain. Overall, this mechanism could thereby fuel the short-term carbon cycle and eventually release ancient carbon to the atmosphere.

5. Conclusion

Compound-specific radiocarbon ages were determined for a suite of plant wax and microbial lipid biomarkers originating from five soils and in sediments from seven different lakes from the Mackenzie River Delta region. The modern to millennial ages of SCFA in the soils reflect a combination of *in situ* production by heterotrophic bacteria and preservation of microbial necromass by mineral interactions. In deeper soil layers, only the millennial pool of SCFA persists, highlighting a stronger role for mineral stabilization. The degree of connectivity of the deltaic lakes to the main river channels, and corresponding amount and frequency of supply of allochthonous organic matter from the Mackenzie River drainage basin, exerts a strong influence on OC in lake sediments. In high closure lakes, which are largely disconnected from the river, the presence of aged SCFA points to *in situ* microbial uptake of pre-aged OC, whereas in low and no closure lakes, pre-aged SCFA likely reflect a combination of *in situ* metabolism and allochthonous supply of pre-aged OC, the latter probably occurring during the spring freshet. Seasonal sampling and in-depth analysis of riverine OC is needed to elucidate sources of pre-aged SCFA. In almost all lake sediment layers, SCFA are younger than LCFA indicating pre-aging of LCFA in soils prior the export to lake sediments. ^{14}C-depleted signatures of specific bacterial biomarker lipids (brGDGTs) provide evidence for the incorporation of old DOC or POC (e.g., permafrost OC) into microbial biomass and its sedimentary residues. The ^{14}C ages of isoGDGT-0 also suggest a heterotrophic source for this archaeal lipid, with the carbon substrate depending on the degree of lake connectivity. However, further data is needed to improve our understanding of heterotrophic archaeal carbon uptake in these environments. Overall, our novel molecular radiocarbon measurements reveal that the incorporation of pre-aged carbon can be traced into microbial lipids and that old organic matter pools may constitute an increasingly important carbon source for lacustrine microbial ecosystems within the Mackenzie Delta with ongoing warming and increased permafrost thaw.

CRediT authorship contribution statement

Julie Lattaud: Writing – original draft, Visualization, Investigation, Funding acquisition, Conceptualization. **Timothy I. Eglinton:** Writing – review & editing, Funding acquisition, Conceptualization. **Negar Haghipour:** Writing – review & editing, Resources. **Marcus Schiedung:** Writing – review & editing, Resources. **Lisa Bröder:** Writing – review & editing, Funding acquisition, Conceptualization.

Data Availability

Data are available at the ETH repository through https://doi.org/10.3929/ethz-b-000697546

Declaration of competing interest

The authors declare that they have no known competing financial interests or personal relationships that could have appeared to influence the work reported in this paper.

Acknowledgments

We thank the sampling team that assisted TE in collecting the sediment cores from the Mackenzie River lakes in 2009 and Jorien Vonk for slicing MD-1 and UD-4. We thank the team that helped sample DIC in winter 2022, Maarten Lupker, Marco Bolandini and Thomas Bossé-Demers. We thank the Laboratory for Ion Beam Physics of ETHZ for support with the AMS ^{14}C measurements. JL was funded by a Rubicon grant (019.183EN.002) from NWO, Netherlands Organization for scientific research. MS was funded by a Swiss National Science Foundation (project 200021_178768). This project received funding from the Swiss Polar Institute and BNP Paribas Swiss Foundation (Project number PAF-2020-004) for the winter 2022 fieldwork. This research has been carried out under the Aurora Research Institute license numbers #14129 (lake sediment cores), #16550 (soils) and #16994 (water DIC) and with the guidance of the Gwich'in Tribal Council (Inuvik).

Appendix A. Supplementary material

The supplementary material contains Figure S1 representing radiocarbon ages and loadings of organic matter in the samples. Table S1 to S5 indicate the mass of compound measured on the AMS, Fm for the DIC, the details for the two end-member modelling and the ETH number of the AMS measurements.

Supplementary material to this article can be found online at https://doi.org/10.1016/j.gca.2025.02.010.

References

Aichner, B., Gierga, M., Stolz, A., Mętrak, M., Wilk, M., Suska-Malawska, M., Mischke, S., Sachse, D., Rajabov, I., Rajabov, N., Rethemeyer, J., 2021. Do radiocarbon ages of plant wax biomarker agree with 14C-TOC/OSL-based age models in an arid high-altitude lake system? Radiocarbon 63, 1575–1590.

ArcticGro, 2024. The Arctic Great Rivers Observatory. Water Quality Dataset.

Bardgett, R.D., Richter, A., Bol, R., Garnett, M.H., Bäumler, R., Xu, X., Lopez-Capel, E., Manning, D.A.C., Hobbs, P.J., Hartley, I.R., Wanek, W., 2007. Heterotrophic microbial communities use ancient carbon following glacial retreat. Biol. Lett. 3, 487–490.

Bird, M.I., Wynn, J.G., Saiz, G., Wurster, C.M., McBeath, A., 2015. The pyrogenic carbon cycle. Annu. Rev. Earth Planet. Sci. 43, 273–298.

Birkholz, A., Smittenberg, R.H., Hajdas, I., Wacker, L., Bernasconi, S.M., 2013. Isolation and compound specific radiocarbon dating of terrigenous branched glycerol dialkyl glycerol tetraethers (brGDGTs). Org Geochem. 60, 9–19.

Blair, N.E., Aller, R.C., 2012. The fate of terrestrial organic carbon in the marine environment. Annu. Rev. Mar. Sci. 4, 401–423.

Blair, N.E., Leithold, E.L., Ford, S.T., Peeler, K.A., Holmes, J.C., Perkey, D.W., 2003. The persistence of memory: the fate of ancient sedimentary organic carbon in a modern sedimentary system. Geochim. Cosmochim. Acta 67, 63–73.

Bonsal, B.R., Kochtubajda, B., 2009. An assessment of present and future climate in the Mackenzie Delta and the near-shore Beaufort Sea region of Canada. Int. J. Climatol. 29, 1780–1795.

Bröder, L., Keskitalo, K.H., Zolkos, S., Shakil, S., Tank, S.E., Kokelj, S.V., Tesi, T., von Dongen, B., Haghipour, N., Eglinton, T.I., 2021. Preferential export of permafrost-derived organic matter as retrogressive thaw slumping intensifies. Environ. Res. Lett. 16, 054059.

Brunauer, S., Emmett, P.H., Teller, E., 1938. Adsorption of gases in multimolecular layers. J. Am. Chem. Soc. 60, 309–319.

Burn, C.R., Kokelj, S.V., 2009. The environment and permafrost of the Mackenzie Delta area. Permafr. Periglac. Process. 20, 83–105.

Chen, L., Liang, J., Qin, S., Liu, L., Fang, K., Xu, Y., Ding, J., Li, F., Luo, Y., Yang, Y., 2016. Determinants of carbon release from the active layer and permafrost deposits on the Tibetan Plateau. Nat. Commun. 7, 13046.

Chen, Y., Zheng, F., Yang, H., Yang, W., Wu, R., Liu, X., Liang, H., Chen, H., Pei, H., Zhang, C., Pancost, R.D., Zeng, Z., 2022. The production of diverse brGDGTs by an Acidobacterium providing a physiological basis for paleoclimate proxies. Geochim. Cosmochim. Acta 337, 155–165.

Cole, J.J., Prairie, Y.T., Caraco, N.F., McDowell, W.H., Tranvik, L.J., Striegl, R.G., Duarte, C.M., Kortelainen, P., Downing, J.A., Middelburg, J.J., Melack, J., 2007. Plumbing the global carbon cycle: integrating inland waters into the terrestrial carbon budget. Ecosystems 10, 172–185.

Dasari, S., Garnett, M.H., Hilton, R.G., 2024. Leakage of old carbon dioxide from a major river system in the Canadian Arctic. PNAS Nexus 3, 134.

Drake, T.W., Wickland, K.P., Spencer, R.G.M., McKnight, D.M., Striegl, R.G., 2015. Ancient low–molecular-weight organic acids in permafrost fuel rapid carbon dioxide production upon thaw. Proc. Natl. Acad. Sci. 112, 13946–13951.

Drake, T.W., Guillemette, F., Hemingway, J.D., Chanton, J.P., Podgorski, D.C., Zimov, N. S., Spencer, R.G.M., 2018. The ephemeral signature of permafrost carbon in an arctic fluvial network. J. Geophys. Res. Biogeosciences 123, 1475–1485.
Drenzek, N.J., Montluçon, D.B., Yunker, M.B., Macdonald, R.W., Eglinton, T.I., 2007. Constraints on the origin of sedimentary organic carbon in the Beaufort Sea from coupled molecular 13C and 14C measurements. Mar. Chem. 103, 146–162.
Drenzek, N.J., Hughen, K.A., Montluçon, D.B., Southon, J.R., dos Santos, G.M., Druffel, E.R.M., Giosan, L., Eglinton, T.I., 2009. A new look at old carbon in active margin sediments. Geology 37, 239–242.
Eglinton, T.I., Eglinton, G., 2008. Molecular proxies for paleoclimatology. Earth Planet. Sci. Lett. 275, 1–16.
Eglinton, T.I., Galy, V.V., Hemingway, J.D., Feng, X., Bao, H., Blattmann, T.M., Dickens, A.F., Gies, H., Giosan, L., Haghipour, N., Hou, P., Lupker, M., McIntyre, C. P., Montluçon, D.B., Peucker-Ehrenbrink, B., Ponton, C., Schefuß, E., Schwab, M.S., Voss, B.M., Wacker, L., Wu, Y., Zhao, M., 2021. Climate control on terrestrial biospheric carbon turnover. Proc. Natl. Acad. Sci. 118, e2011585118.
Elberling, B., Michelsen, A., Schädel, C., Schuur, E.A.G., Christiansen, H.H., Berg, L., Tamstorf, M.P., Sigsgaard, C., 2013. Long-term CO_2 production following permafrost thaw. Nat. Clim. Chang. 3, 890–894.
Emmerton, C.A., Lesack, L.F.W., Marsh, P., 2007. Lake abundance, potential water storage, and habitat distribution in the Mackenzie River Delta, western Canadian Arctic. Water Resour. Res. 43, 1–14.
Feng, X., Gustafsson, Ö., Holmes, R.M., Vonk, J.E., von Dongen, B., Semiletov, I.P., Dudarev, O.V., Yunker, M.B., MacDonald, R.W., Wacker, L., Montlucon, D., Eglinton, T.I., 2015. Multimolecular tracers of terrestrial carbon transfer across the pan-Arctic: 14C characteristics of sedimentary carbon components and their environmental controls. Glob. Biogeochem. Cycles 29, 1855–1873.
Ferguson, M.E., 1990. Sediment movement in lakes in the centra area of the Mackenzie delta, N.W.T.
Freymond, C.V., Kündig, N., Stark, C., Peterse, F., Buggle, B., Lupker, M., Plötze, M., Blattmann, T.M., Filip, F., Giosan, L., Eglinton, T.I., 2018. Evolution of biomolecular loadings along a major river system. Geochim. Cosmochim. Acta 223, 389–404.
Gierga, M., Hajdas, I., van Raden, U.J., Gilli, A., Wacker, L., Sturm, M., Bernasconi, S.M., Smittenberg, R.H., 2016. Long-stored soil carbon released by prehistoric land use: evidence from compound-specific radiocarbon analysis on Soppensee lake sediments. Quat. Sci. Rev. 144, 123–131.
Gies, H., Hagedorn, F., Lupker, M., Montluçon, D., Haghipour, N., Van Der Voort, T.S., Eglinton, T.I., 2021. Millennial-age glycerol dialkyl glycerol tetraethers (GDGTs) in forested mineral soils: 14C-based evidence for stabilization of microbial necromass. Biogeosciences 18, 189–205.
Gies, H., Lupker, M., Galy, V., Hemingway, J., Boehman, B., Schwab, M., Haghipour, N., Eglinton, T.I., 2023. Multi-molecular 14C evidence for mineral control on terrestrial carbon storage and export. Philos. Trans. r. Soc. Math. Phys. Eng. Sci. 381, 20220328.
Goñi, M.A., Yunker, M.B., MacDonald, R.W., Eglinton, T.I., 2005. Distribution and sources of organic biomarkers in arctic sediments from the Mackenzie River and Beaufort Shelf. Mar. Chem. 71, 23–51.
Gorham, E., Lehman, C., Dyke, A., Janssens, J., Dyke, L., 2007. Temporal and spatial aspects of peatland initiation following deglaciation in North America. Quat. Sci. Rev. 26, 300–311.
Graham, D.E., Wallenstein, M.D., Vishnivetskaya, T.A., Waldrop, M.P., Phelps, T.J., Pfiffner, S.M., Onstott, T.C., Whyte, L.G., Rivkina, E.M., Gilichinsky, D.A., Elias, D. A., Mackelprang, R., VerBerkmoes, N.C., Hettich, R.L., Wagner, D., Wullschleger, S. D., Jansson, J.K., 2012. Microbes in thawing permafrost: the unknown variable in the climate change equation. ISME J. 6, 709–712.
Gruber, S., 2012. Derivation and analysis of a high-resolution estimate of global permafrost zonation. Cryosphere 6, 221–233.
Guillemette, F., Bianchi, T.S., Spencer, R.G.M., 2017. Old before your time: ancient carbon incorporation in contemporary aquatic foodwebs. Limnol. Oceanogr. 62, 1682–1700.
Haghipour, N., Ausin, B., Usman, M.O., Ishikawa, N., Wacker, L., Welte, C., Ueda, K., Eglinton, T.I., 2018. Compound-specific radiocarbon analysis by elemental analyzer–accelerator mass spectrometry: precision and limitations. Anal. Chem. 91, 2042–2049.
Halamka, T.A., Raberg, J.H., McFarlin, J.M., Younkin, A.D., Mulligan, C., Liu, X.-L., Kopf, S.H., 2023. Production of diverse brGDGTs by Acidobacterium Solibacter usitatus in response to temperature, pH, and O2 provides a culturing perspective on brGDGT proxies and biosynthesis. Geobiology 21, 102–118.
Hemingway, J.D., Rothman, D.H., Grant, K.E., Rosengard, S.Z., Eglinton, T.I., Derry, L.A., Galy, V.V., 2019. Mineral protection regulates long-term global preservation of natural organic carbon. Nature 570, 228–231.
Hilton, R.G., Galy, V., Gaillardet, J., Dellinger, M., Bryant, C., O'Regan, M., Gröcke, D.R., Coxall, H., Bouchez, J., Calmels, D., 2015. Erosion of organic carbon in the Arctic as a geological carbon dioxide sink. Nature 524, 84–87.
Holmes, R.M., McClelland, J.W., Raymond, P.A., Frazer, B.B., Peterson, B.J., Stieglitz, M., 2008. Lability of DOC transported by Alaskan rivers to the Arctic Ocean. Geophys. Res. Lett. 35.
Horan, K., Hilton, R.G., Dellinger, M., Tipper, E.D., Galy, V., Calmels, D., Selby, D., Burton, K.W., 2019. Carbon dioxide emission by rock organic carbon oxidation and the net geochemical carbon budget of the Mackenzie River basin. Am. J. Sci. 319, 473–499.
Jasper, J.P., Gagosian, R.B., 1993. The relationship between sedimentary organic carbon isotopic composition and organic biomarker compound concentration. Geochim. Cosmochim. Acta 57, 167–186.
Kabanov, P., Gouwy, S.A., 2017. The Devonian Horn River Group and the basal Imperial Formation of the central Mackenzie Plain, N.W.T., Canada: multiproxy stratigraphic framework of a black shale basin. Can. J. Earth Sci. 54, 409–429.
Keil, R.G., Montluçon, D.B., Prahl, F.G., Hedges, J.I., 1994. Sorptive preservation of labile organic matter in marine sediments. Nature 370, 549–552.
Keil, R.G., Mayer, L.M., Quay, P.D., Richey, J.E., Hedges, J.I., 1997. Loss of organic matter from riverine particles in deltas. Geochim. Cosmochim. Acta 61, 1507–1511.
Keskitalo, K.H., Bröder, L., Shakil, S., Zolkos, S., Tank, S.E., van Dongen, B.E., Tesi, T., Haghipour, N., Eglinton, T.I., Kokelj, S.V., Vonk, J.E., 2021. Downstream evolution of particulate organic matter composition from permafrost thaw slumps. Front. Earth Sci. 9.
Kusch, S., Mollenhauer, G., Willmes, C., Hefter, J., Eglinton, T.I., Galy, V., 2021. Controls on the age of plant waxes in marine sediments – a global synthesis. Org Geochem. 157, 104259.
Lattaud, J., Bröder, L., Haghipour, N., Rickli, J., Giosan, L., Eglinton, T.I., 2021a. Influence of hydraulic connectivity on carbon burial efficiency in Mackenzie Delta lake sediments. J. Geophys. Res. Biogeosciences 126.
Lattaud, J., De Jonge, C., Elling, F.J., Pearson, A., Eglinton, T.I., 2021b. Microbial lipid signatures in Arctic deltaic sediments – insights into methane cycling and climate variability. Org Geochem. 157.
Lesack, L.F.W., Marsh, P., 2007. Lengthening plus shortening of river-to-lake connection times in the Mackenzie River Delta respectively via two global change mechanisms along the arctic coast. Geophys. Res. Lett. 34, 1–6.
Liu, F., Kou, D., Abbott, B.W., Mao, C., Chen, Y., Chen, L., Yang, Y., 2019. Disentangling the effects of climate, vegetation, soil and related substrate properties on the biodegradability of permafrost-derived dissolved organic carbon. J. Geophys. Res. Biogeosciences 124, 3377–3389.
Mann, P.J., Davydova, A., Zimov, N., Spencer, R.G.M., Davydov, S., Bulygina, E., Zimov, S., Holmes, R.M., 2012. Controls on the composition and lability of dissolved organic matter in Siberia's Kolyma River basin. J. Geophys. Res. Biogeosciences 117.
Mann, P.J., Eglinton, T.I., McIntyre, C.P., Zimov, N., Davydova, A., Vonk, J.E., Holmes, R.M., Spencer, R.G.M., 2015. Utilization of ancient permafrost carbon in headwaters of Arctic fluvial networks. Nat. Commun. 6, 7856.
Matsumoto, K., Kawamura, K., Uchida, M., Shibata, Y., 2007. Radiocarbon content and stable carbon isotopic ratios of individual fatty acids in subsurface soil: Implication for selective microbial degradation and modification of soil organic matter. Geochem. J. 41, 483–492.
McIntyre, C., Wacker, L., Haghipour, N., Blattmann, T.M., Fahrni, S., Usman, M.O., Eglinton, T.I., Synal, H.-A., 2016. Online 13C and 14C gas measurements by EA-IRMS–AMS at ETH Zürich. Radiocarbon 59, 893–903.
Miesner, F., Overduin, P.P., Grosse, G., Strauss, J., Langer, M., Westermann, S., Schneider von Deimling, T., Brovkin, V., Arndt, S., 2023. Subsea permafrost organic carbon stocks are large and of dominantly low reactivity. Sci. Rep. 13, 9425.
O'Neill, H.B., Smith, S.L., Duchesne, C., 2019. Long-Term Permafrost Degradation and Thermokarst Subsidence in the Mackenzie Delta Area Indicated by Thaw Tube Measurements 643–651. https://doi.org/10.1061/9780784482599.074.
Parker, W.G., Ahad, J.M.E., Obrist-Farner, J., Keenan, B., Douglas, P.M.J., 2023. Distinct modes of aged soil carbon export in a large tropical lake basin identified using bulk and compound-specific radiocarbon analyses of fluvial and lacustrine sediment. J. Geophys. Res Biogeosci. 128 e2023JG007515.
Petsch, S.T., Eglinton, T.I., Edwards, K.J., 2001. 14C-dead living biomass: evidence for microbial assimilation of Ancient organic carbon during shale weathering. Science 292, 1127–1131.
Reiffarth, D.G., Petticrew, E.L., Owens, P.N., Lobb, D.A., 2016. Sources of variability in fatty acid (FA) biomarkers in the application of compound-specific stable isotopes (CSSIs) to soil and sediment fingerprinting and tracing: a review. Sci. Total Environ. 565, 8–27.
Rieb, E.C., Polik, C.A., Ward, C.P., Kling, G.W., Cory, R.M., 2024. Controls on the respiration of ancient carbon draining from permafrost soils into sunlit Arctic surface waters. J. Geophys. Res Biogeosci. 129, e2023JG007853.
Ruben, M., Hefter, J., Schubotz, F., Geibert, W., Butzin, M., Gentz, T., Grotheer, H., Forwick, M., Szczuciński, W., Mollenhauer, G., 2023. Fossil organic carbon utilization in marine Arctic fjord sediments by subsurface micro-organisms. Nat. Geosci. 16, 625–630.
Ruben, M., Marchant, H., Wietz, M., Gentz, T., Strauss, J., Koch, B.P., Mollenhauer, G., 2024. Microbial communities degrade ancient permafrost-derived organic matter in Arctic seawater. J. Geophys. Res Biogeosci. 129, e2023JG007936.
Ruff, M., Fahrni, S., Gäggeler, H.W., Hajdas, I., Suter, M., Synal, H.-A., Szidat, S., Wacker, L., 2010. On-line radiocarbon measurements of small samples using elemental analyzer and MICADAS gas ion source. Radiocarbon 52, 1645–1656.
Sauer, P.E., Eglinton, T.I., Schimmelmann, A., Hayes, J.M., Sessions, A.L., 2001. Compound-specific D/H ratios of lipid biomarkers from sediments as a proxy for environmental and climatic conditions. Geochim. Cosmochim. Acta 65, 213–222.
Schädel, C., Schuur, E.A.G., Bracho, R., Elberling, B., Knoblauch, C., Lee, H., Luo, Y., Shaver, G.R., Turetsky, M.R., 2014. Circumpolar assessment of permafrost C quality and its vulnerability over time using long-term incubation data. Glob. Chang. Biol. 20, 641–652.
Schiedung, M., Bellè, S.-L., Malhotra, A., Abiven, S., 2022. Organic carbon stocks, quality and prediction in permafrost-affected forest soils in North Canada. Catena 213, 106194.
Schiedung, M., Ascough, P., Bellè, S.-L., Bird, M.I., Bröder, L., Haghipour, N., Hilton, R. G., Lattaud, J., Abiven, S., 2024. Millennial-aged pyrogenic carbon in high-latitude mineral soils. Commun. Earth Environ. 5, 177.
Schouten, S., Hopmans, E.C., Damsté, J.S.S., Sinninghe Damsté, J.S., 2013. The organic geochemistry of glycerol dialkyl glycerol tetraether lipids: a review. Org Geochem. 54, 19–61.

Schuur, E.A.G., Carbone, M.S., Hicks Pries, C.E., Hopkins, F.M., Natali, S.M., 2016. Radiocarbon in Terrestrial Systems. In: Schuur, E.A.G., Druffel, E., Trumbore, S.E. (Eds.), Radiocarbon and Climate Change: Mechanisms, Applications and Laboratory Techniques. Springer International Publishing, Cham, pp. 167–220.

Schuur, E. a. G., McGuire, A.D., Schädel, C., Grosse, G., Harden, J.W., Hayes, D.J., Hugelius, G., Koven, C.D., Kuhry, P., Lawrence, D.M., Natali, S.M., Olefeldt, D., Romanovsky, V.E., Schaefer, K., Turetsky, M.R., Treat, C.C., Vonk, J.E., 2015. Climate change and the permafrost carbon feedback. Nature 520, 171–179. https://doi.org/10.1038/nature14338.

Schuur, E.A.G., Hicks Pries, C., Mauritz, M., Pegoraro, E., Rodenhizer, H., See, C., Ebert, C., 2023. Ecosystem and soil respiration radiocarbon detects old carbon release as a fingerprint of warming and permafrost destabilization with climate change. Philos. Trans. r. Soc. Math. Phys. Eng. Sci. 381, 20220201.

Schwab, M.S., Hilton, R.G., Raymond, P.A., Haghipour, N., Amos, E., Tank, S.E., Holmes, R.M., Tipper, E.T., Eglinton, T.I., 2020. An abrupt aging of dissolved organic carbon in large Arctic rivers. Geophys. Res. Lett. 47, e2020GL088823.

Shah, S.R., Pearson, A., 2007. Ultra-microscale (5–25 μg C) analysis of individual lipids by 14C AMS: assessment and correction for sample processing blanks. Radiocarbon 49, 69–82.

Simoneit, B.R.T., 2005. A review of current applications of mass spectrometry for biomarker/molecular tracer elucidations. Mass Spectrom. Rev. 24, 719–765.

Smittenberg, R.H., Baas, M., Green, M.J., Hopmans, E.C., Schouten, S., Sinninghe Damsté, J.S., 2005. Pre- and post-industrial environmental changes as revealed by the biogeochemical sedimentary record of Drammensfjord. Norway. Mar. Geol. 214, 177–200.

Squires, M.M., Lesack, L.F.W., 2002. Water transparency and nutrients as controls on phytoplankton along a flood-frequency gradient among lakes of the Mackenzie Delta, western Canadian Arctic. Can. J. Fish. Aquat. Sci. 59, 1339–1349.

Stuiver, M., Polach, H.A., 1977. Discussion reporting of 14C data. Radiocarbon 19, 355–363.

Synal, H.-A., Stocker, M., Suter, M., 2007. MICADAS: a new compact radiocarbon AMS system. Nucl. Instrum. Methods Phys. Res. Sect. B Beam Interact. Mater. At Accelerator Mass Spectrometry 259, 7–13.

Tank, S.E., Lesack, L.F.W., Gareis, J.A.L., Osburn, C.L., Hesslein, R.H., 2011. Multiple tracers demonstrate distinct sources of dissolved organic matter to lakes of the Mackenzie Delta, Western Canadian Arctic. Limnol. Oceanogr. 56, 1297–1309.

Tranvik, L.J., Downing, J.A., Cotner, J.B., Loiselle, S.A., Striegl, R.G., Ballatore, T.J., Dillon, P., Finlay, K., Fortino, K., Knoll, L.B., Kortelainen, P.L., Kutser, T., Larsen, S., Laurion, I., Leech, D.M., Leigh McCallister, S., McKnight, D.M., Melack, J.M., Overholt, E., Porter, J.A., Prairie, Y., Renwick, W.H., Roland, F., Sherman, B.S., Schindler, D.W., Sobek, S., Tremblay, A., Vanni, M.J., Verschoor, A.M., Von Wachenfeldt, E., Weyhenmeyer, G.A., 2009. Lakes and reservoirs as regulators of carbon cycling and climate. Limnol. Oceanogr. 54, 2298–2314.

Treat, C., Jones, M.C., 2018. Near-surface permafrost aggradation in Northern Hemisphere peatlands shows regional and global trends during the past 6000 years. The Holocene 28, 998–1010.

Trumbore, S., 2009. Radiocarbon and soil carbon dynamics. Annu. Rev. Earth Planet. Sci. 37, 47–66.

Uchikawa, J., Popp, B.N., Schoonmaker, J.E., Xu, L., 2008. Direct application of compound-specific radiocarbon analysis of leaf waxes to establish lacustrine sediment chronology. J. Paleolimnol. 39, 43–60.

Van Der Voort, T.S., Zell, C.I., Hagedorn, F., Feng, X., McIntyre, C.P., Haghipour, N., Graf Pannatier, E., Eglinton, T.I., 2017. Diverse soil carbon dynamics expressed at the molecular level. Geophys. Res. Lett. 44.

Vonk, J.E., Giosan, L., Blusztajn, J., Montlucon, D., Graf Pannatier, E., McIntyre, C., Wacker, L., Macdonald, R.W., Yunker, M.B., Eglinton, T.I., 2015. Spatial variations in geochemical characteristics of the modern Mackenzie Delta sedimentary system. Geochim. Cosmochim. Acta 171, 100–120.

Vonk, J.E., Dickens, A.F., Giosan, L., Hussain, Z.A., Kim, B., Zipper, S.C., Holmes, R.M., Montlucon, D.B., Galy, V., Eglinton, T.I., 2016. Arctic deltaic lake sediments as recorders of fluvial organic matter deposition. Front. Earth Sci. 4, 1–24.

Vonk, J.E., Drenzek, N.J., Hughen, K.A., Stanley, R.H.R., McIntyre, C., Montluçon, D.B., Giosan, L., Southon, J.R., Santos, G.M., Druffel, E.R.M., Andersson, A.A., Sköld, M., Eglinton, T.I., 2019. Temporal deconvolution of vascular plant-derived fatty acids exported from terrestrial watersheds. Geochim. Cosmochim. Acta 244, 502–521.

Wacker, L., Bonani, G., Friedrich, M., Hajdas, I., Kromer, B., Němec, M., Ruff, M., Suter, M., Synal, H.-A., Vockenhuber, C., 2010. MICADAS: routine and high-precision radiocarbon dating. Radiocarbon 52, 252–262.

Weijers, J.W.H., Wiesenberg, G.L.B., Bol, R., Hopmans, E.C., Pancost, R.D., 2010. Carbon isotopic composition of branched tetraether membrane lipids in soils suggest a rapid turnover and a heterotrophic life style of their source organism(s). Biogeosciences 7, 2959–2973.

Wiesenberg, G.L.B., Gocke, M., Kuzyakov, Y., 2010. Fast incorporation of root-derived lipids and fatty acids into soil – Evidence from a short term multiple 14CO2 pulse labelling experiment. Org. Geochem., Advances in Organic Geochemistry 2009 41, 1049–1055. https://doi.org/10.1016/j.orggeochem.2009.12.007.

Wild, B., Andersson, A., Bröder, L., Vonk, J., Hugelius, G., McClelland, J.W., Song, W., Raymond, P.A., Gustafsson, Ö., 2019. Rivers across the Siberian Arctic unearth the patterns of carbon release from thawing permafrost. Proc. Natl. Acad. Sci. 116, 10280–10285.

Yunker, M.B., Macdonald, R.W., Cretney, W.J., Fowler, B.R., McLaughlin, F.A., 1993. Alkane, terpene and polycyclic aromatic hydrocarbon geochemistry of the Mackenzie River and Mackenzie shelf: riverine contributions to Beaufort Sea coastal sediment. Geochim. Cosmochim. Acta 57, 3041–3061.

Yunker, M.B., Backus, S.M., Graf Pannatier, E., Jeffries, D.S., Macdonald, R.W., 2002. Sources and significance of alkane and PAH hydrocarbons in Canadian Arctic Rivers. Estuar. Coast. Shelf Sci. 55, 1–31.